Supporting Information for

Efficient plasmonic water splitting by heteroepitaxial junction-induced faceting of gold nanoparticles on anatase titanium(IV) oxide nanoplate array electrode

Shin-ichi Naya,[a] Yoko Morita,[b] Hisashi Sugime,[b,c]

Tetsuro Soejima,[b,c] Musashi Fujishima,[b,c] Hiroaki Tada[d]*

[a] Environmental Research Laboratory, Kindai University, 3-4-1, Kowakae, Higashi-Osaka, Osaka 577-8502, Japan.

[b] Graduate School of Science and Engineering, Kindai University, 3-4-1, Kowakae, Higashi-Osaka, Osaka 577-8502, Japan.

[c] Department of Applied Chemistry, Faculty of Science and Engineering, Kindai University, 3-4-1, Kowakae, Higashi-Osaka, Osaka 577-8502, Japan.

[d] Institutes of Innovation for Future Society, Nagoya University, Furo-cho, Chikusa-ku, Nagoya 464-8603, Japan.

* To whom correspondence should be addressed: Prof. Hiroaki Tada

E-mail: hiroaki.tada@mirai.nagoya-u.ac.jp

Table of Contents

Table S1. IPCE for water splitting on Au plasmonic photocatalyst electrodes

Plasmonic metal	Size	Semiconductor electrode	Crsytal form of TiO_2	IPCE (%)	Wavelength	Ref.
Au	5.2 nm	TiO_2 NWA	anatase	0.03	520 nm	18
Au	4.7 nm	mp-TiO_2	anatase	2.6×10^{-3}	560 nm	21
Au	5 nm	mp-TiO_2	rutile	3×10^{-4}	600 nm	22
Au	< 20 nm	TiO_2 NWA	rutile	~0.03	520 nm	23
Au	7.6	TiO_2 NPLA	anatase	0.39	600 nm	This work
Au	6.2	TiO_2 NWA	rutile	0.18	600 nm	This work

Reference

18. H. Li, S. Wang, M. Wang, Y. Gao, J. Tang, S. Zhao, H. Chi, P. Zhang, J. Qu, F. Fan and C. Li, Enhancement of Plasmon-Induced Photoelectrocatalytic Water Oxidation over Au/TiO_2 with Lithium Intercalation, *Angew. Chem. Int. Ed.*, 2022, **61**, e202204272.
21. P. A. DeSario, J. J. Pietron, D. E. DeVantier, T. H. Brintlinger, R. M. Stroud and D. R. Rolison, Plasmonic enhancement of visible-light water splitting with Au–TiO_2 composite aerogels, *Nanoscale*, 2013, **5**, 8079-8083.
22. T. Onishi, M. Teranishi, S. Naya, M. Fujishima and H. Tada, Electrocatalytic effect on the photon−to−current conversion efficiency of gold−nanoparticle−loaded titanium(IV) oxide plasmonic electrode for water oxidation, *J. Phys. Chem. C*, 2020, **124**, 6103-6109.
23. S.-F. Hung, F.-X. Xiao, Y.-Y. Hsu, N.-T. Suen, H.-B. Yang, H. M. Chen and B. Liu, Iridium oxide-assisted plasmon-induced hot carriers: Improvement on kinetics and thermodynamics of hot carriers, *Adv. Energy Mater.*, 2016, **6**, 1501339.

Table S2. EIS parameters for Au/TiO_2 plasmonic Electrodes [a]

	R_s / Ω	CPE α	CPE C_0	R_{ct} / Ω
DP-Au/A-TiO_2 NPLA	4.9×10	7.5×10^{-1}	8.1×10^{-5}	1.3×10^{3}
DP-Au/R-TiO_2 NWA	4.4×10	8.5×10^{-1}	5.0×10^{-6}	9.0×10^{3}
CR-Au/A-TiO_2 NPLA	9.3×10	9.3×10^{-1}	4.5×10^{-5}	2.4×10^{5}

[a] Constant phase element (CPE) is expressed by the equation $ZCPE = 1/C_0(j\omega)^{\alpha}$.

Table S3. Maximum enhancement factors ($|E|^2/|E_0|^2$) calculated for HS-Au/A-TiO_2, t-Oh-Au/A-TiO_2, and t-Oh-Au/R-TiO_2 at the LSPR peak wavelengths by the 3D-FDTD method

Model	d / nm	λ / nm	Monitor plane	Maximum E/E_0	Maximum $\|E\|^2/\|E_0\|^2$
HS-Au/A-TiO_2	7.9	702	xz	49.6	2.5×10^3
			xy	59.9	3.6×10^3
t-Oh-Au/A-TiO_2	7.6	617	*xz*	91.6	8.4×10^3
			xy	192	3.7×10^4
		637	*xz*	254	6.5×10^4
			xy	292	8.5×10^4
		650	*xz*	331	1.1×10^5
			xy	333	1.1×10^5
		670	*xz*	103	1.1×10^4
			xy	336	1.1×10^5
t-Oh-Au/R-TiO_2	6.2	672	*xz*	340	1.2×10^5
			xy	340	1.2×10^5
		706	*xz*	116	1.4×10^4
			xy	383	1.5×10^5

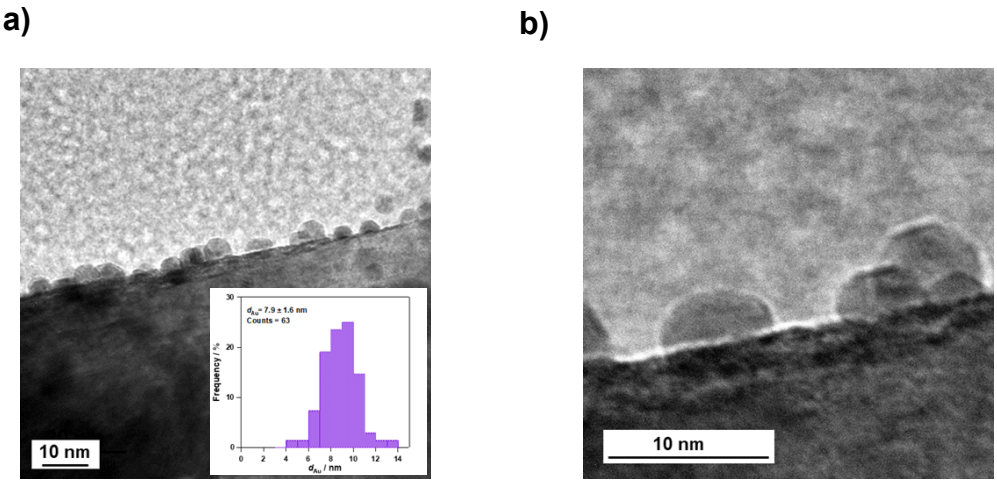

Fig. S1. (a) TEM image and Au particle size distribution (a) and HR-TEM image (b) of CR-Au/A-TiO_2 NPLA.

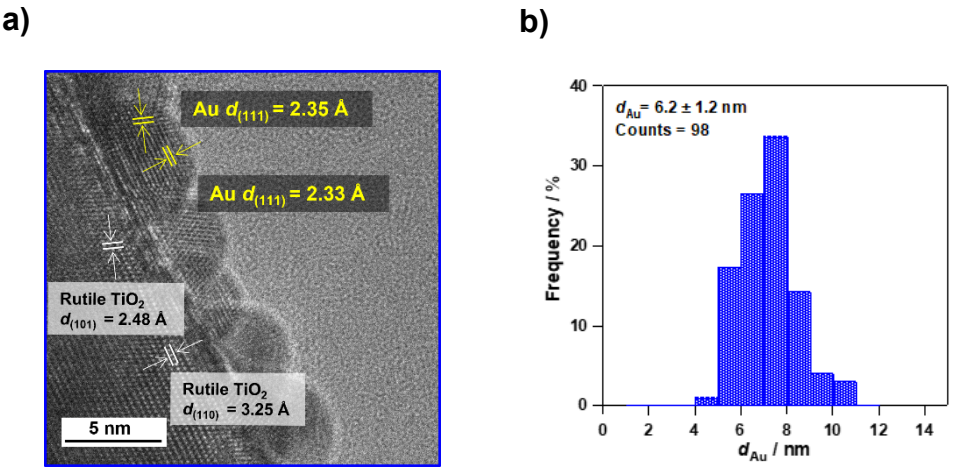

Fig. S2. HR-TEM image (a) and Au particle size distribution (b) of DP-Au/R-TiO_2 NWA.

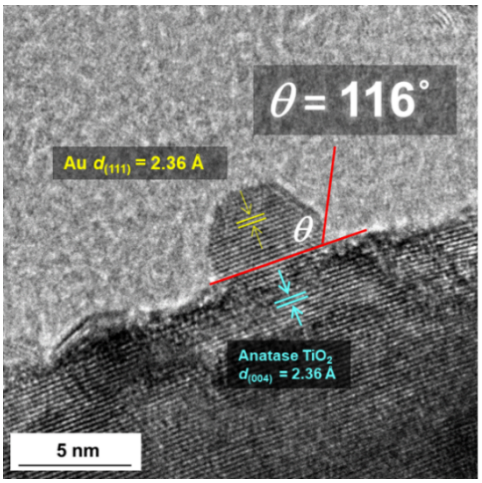

Fig. S3. Contact angle of Au NP on the A-TiO_2(001) surface.

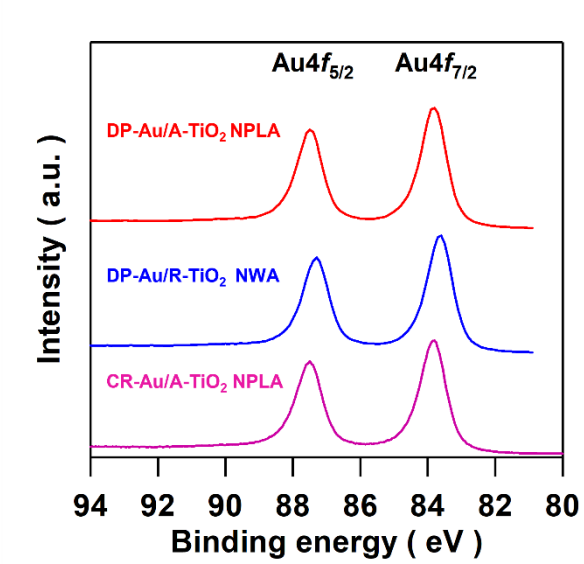

Fig. S4. Au4f XP spectra of DP-Au/A-TiO_2 NPLA, DP-Au/R-TiO_2 NWA, and CR-Au/A-TiO_2 NPLA.

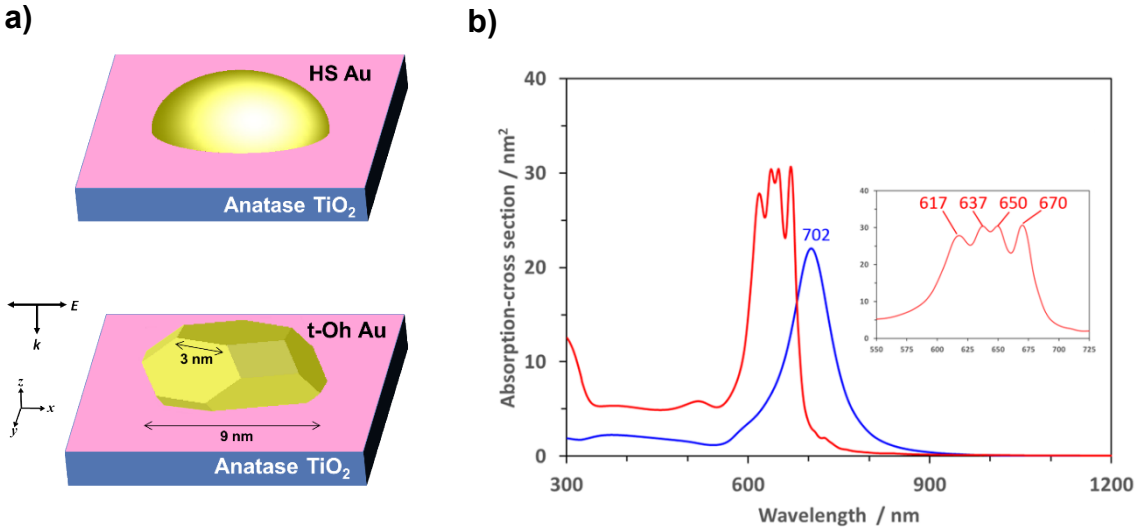

Fig. S5. (a) FDTD calculation models for CR-Au/A-TiO_2 (HS-Au/A-TiO_2) and DP-Au/A-TiO_2 NPLA (t-Oh-Au/A-TiO_2) (b) FDTD-simulated absorption spectra of the HS-Au/A-TiO_2 (blue) and t-Oh-Au/A-TiO_2 (red).

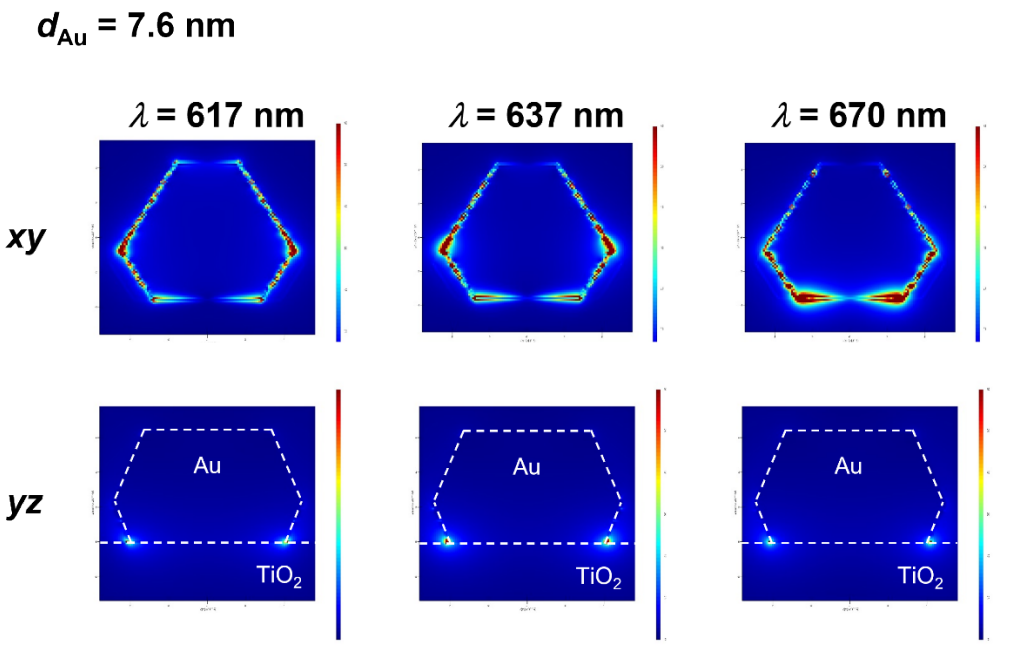

Fig. S6. Local electric field distribution for t-Oh-Au(d_{Au} = 7.6 nm)/A-TiO_2 calculated by the 3D-FDTD method.

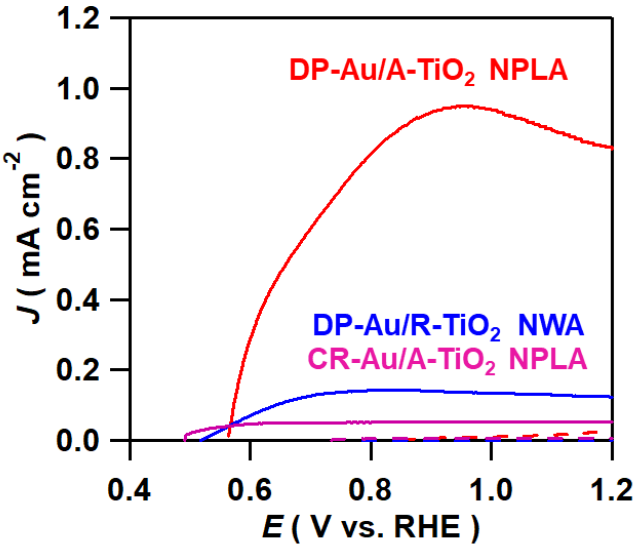

Fig. S7. Photocurrent (*J*)-potential (*E*) curves of DP-Au/A-TiO_2 NPLA and DP-Au/R-TiO_2 NWA electrodes. The current density in each system was calculated using the specific surface area of the nanostructured TiO_2 determined by the BET method.

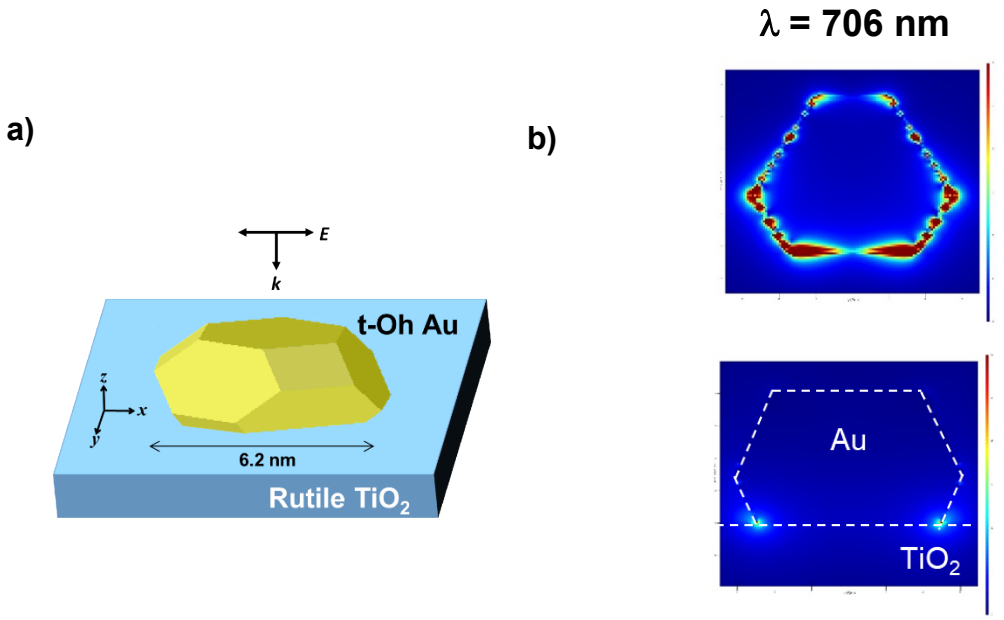

Fig. S8. Local electric fields for t-Oh-Au/R-TiO_2 (a) calculated by the 3D-FDTD method, and the local electric field distributions (b).